Biochimica et Biophysica Acta 1808 (2011) 65–77

Contents lists available at ScienceDirect

Biochimica et Biophysica Acta

journal homepage: www.elsevier.com/locate/bbamem

Characterisation of the purified human sodium/iodide symporter reveals that the protein is mainly present in a dimeric form and permits the detailed study of a native C-terminal fragment

Sylvaine Huc-Brandt [a,1,2], Didier Marcellin [a,1], Fanny Graslin [b], Olivier Averseng [a], Laurent Bellanger [a], Patrick Hivin [a,3], Eric Quemeneur [a], Cécile Basquin [b,4], Valérie Navarro [b], Thierry Pourcher [b], Elisabeth Darrouzet [a,*]

[a] CEA, iBEB, SBTN, Centre de Marcoule, Bat 170, BP17171, 30207 Bagnols sur Cèze, CEDEX, France
[b] TIRO laboratory, CEA/Centre Antoine Lacassagne/University of Nice Sophia-Antipolis, School of Medicine, 28 Avenue de Valombrose, 06107 Nice, France

ARTICLE INFO

Article history:
Received 29 March 2010
Received in revised form 16 August 2010
Accepted 18 August 2010
Available online 23 August 2010

Keywords:
Thyroid
Sodium/iodide symporter
Membrane protein
Eukaryote
Oligomeric state
Post-translational regulation

ABSTRACT

The sodium/iodide symporter is an intrinsic membrane protein that actively transports iodide into thyroid follicular cells. It is a key element in thyroid hormone biosynthesis and in the radiotherapy of thyroid tumours and their metastases. Sodium/iodide symporter is a very hydrophobic protein that belongs to the family of sodium/solute symporters. As for many other membrane proteins, particularly mammalian ones, little is known about its biochemistry and structure. It is predicted to contain 13 transmembrane helices, with an N-terminus oriented extracellularly. The C-terminal, cytosolic domain contains approximately one hundred amino acid residues and bears most of the transporter's putative regulatory sites (phosphorylation, sumoylation, di-acide, di-leucine or PDZ-binding motifs). In this study, we report the establishment of eukaryotic cell lines stably expressing various human sodium/iodide symporter recombinant proteins, and the development of a purification protocol which allowed us to purify milligram quantities of the human transporter. The quaternary structure of membrane transporters is considered to be essential for their function and regulation. Here, the oligomeric state of human sodium/iodide symporter was analysed for the first time using purified protein, by size exclusion chromatography and light scattering spectroscopy, revealing that the protein exists mainly as a dimer which is stabilised by a disulfide bridge. In addition, the existence of a sodium/iodide symporter C-terminal fragment interacting with the protein was also highlighted. We have shown that this fragment exists in various species and cell types, and demonstrated that it contains the amino-acids [512–643] from the human sodium/iodide symporter protein and, therefore, the last predicted transmembrane helix. Expression of either the [1–512] truncated domain or the [512–643] domain alone, as well as co-expression of the two fragments, was performed, and revealed that co-expression of [1–512] with [512–643] allowed the reconstitution of a functional protein. These findings constitute an important step towards an understanding of some of the post-translational mechanisms that finely tune iodide accumulation through human sodium/iodide symporter regulation.

Abbreviations: BCA, bicinchoninic acid; C12E8, octaethylene glycol monododecyl ether; CMV, cytomegalovirus; DAB, 3,3′-diaminobenzidine; DDM, n-dodecyl β-D-maltoside; HEK, human embryonic kidney cells; HEPES, 4-(2-Hydroxyethyl)piperazine-1-ethanesulfonic acid; IMAC, immobilized metal affinity chromatography; LDS, Lithium dodecylsulfate; MES, 4-morpholineethanesulfonic acid; MOPS, 4-morpholinepropanesulfonic acid; PAGE, polyacrylamide gel electrophoresis; SEC, size exclusion chromatography; Tris, 2-Amino-2-(hydroxymethyl)-1,3–propanediol; TX–100, Triton X100

* Corresponding author. Tel.: +33 4 66 79 19 16; fax: +33 4 66 79 19 05.
E-mail addresses: sylvaine.huc@igf.cnrs.fr (S. Huc-Brandt), didier.marcellin@cea.fr (D. Marcellin), fanny.graslin@unice.fr (F. Graslin), olivier.averseng@cea.fr (O. Averseng), laurent.bellanger@cea.fr (L. Bellanger), patrick.hivin@deinove.com (P. Hivin), eric.quemeneur@cea.fr (E. Quemeneur), cecile.basquin@einstein.yu.edu (C. Basquin), navarro_valerie@yahoo.fr (V. Navarro), thierry.pourcher@unice.fr (T. Pourcher), elisabeth.darrouzet@cea.fr (E. Darrouzet).
[1] Both authors contributed equally this work.
[2] Present address: Institute of Functional Genomics, CNRS UMR5203, INSERM U661, UM1, UM2, Physiology Department, 141, rue de la Cardonille, 34.094 Montpellier cedex 5, France.
[3] Present address: Deinove, Cap Alpha, Avenue de l'Europe, Clapiers, 34940 Montpellier CEDEX 09, France.
[4] Present address: Department of Molecular Pharmacology, Albert Einstein College of Medicine, Forchheimer building, room 209,1300 Morris Park Ave,Bronx, NY 10461, USA.

0005-2736/$ – see front matter © 2010 Elsevier B.V. All rights reserved.
doi:10.1016/j.bbamem.2010.08.013

1. Introduction

The sodium/iodide symporter (NIS) is an intrinsic membrane protein that uses the sodium gradient to actively transport iodide into thyroid follicular cells, representing a key element in thyroid hormone biosynthesis [1–3]. Its properties are widely exploited for the radiotherapy of thyroid tumours and their metastases, and its expression by gene therapy could broaden further its use in medical applications [2–5]. The human and rat NIS genes were cloned and sequenced more than ten years ago and, more-recently, the mouse equivalent [6–8]. NIS belongs to the family of sodium/solute symporters, such as the sodium/proline or sodium/glucose symporters [9]. Human NIS is a 643 amino acid protein, predicted to contain 13 transmembrane helices, with the N-terminus oriented extracellularly and the C-terminus (of nearly one hundred amino-acids) facing the cytosol [10]. NIS is finely regulated at the transcriptional and post-translational level. However, whereas much is known about its regulation at the transcriptional level, few data are available concerning its post-translational regulation at the molecular level [3,5,11–15]. Many membrane proteins, especially transporters, exist as multimeric complexes [16–18]. Some of these oligomeric forms serve a function for stability, but in other cases they are also required for catalytic function. For example, both the sodium bicarbonate co-transporter and the sodium/proton exchanger are found in oligomeric states but their functional units are monomers, whereas the minimum functional unit for the multidrug EmrE or the calcium-ATPase is a dimer [19–22]. Many studies have investigated the oligomeric state of the sodium-dependent neurotransmitter transporters in respect to their function or their trafficking, and it has been shown that the oligomeric state is a prerequisite in passing quality control in the endoplasmic reticulum [23]. In the case of GPCRs (G protein-coupled receptors), the complexity increases with the formation of hetero-multimers [24]. The supramolecular assembly of membrane proteins is therefore an important field of study, in acquiring a better understanding of their regulation. In addition the C-terminal region of hNIS comprises a rather hydrophilic domain that represents the longer stretch of amino-acids predicted to lie outside the membrane. It is, therefore, not surprising to encounter in this region most of the bioinformatically-predicted or biochemically-proven regulatory sites of the protein: phosphorylation, sumoylation, di-acid, di-leucine and PDZ-binding motifs [11,13]. This domain may also be involved in the symporter protein–protein interactions. A study on hNIS truncated forms (variants 531X or 515X) associated with iodide uptake deficiency, as well as two studies based on chimeric constructs between human and murine transporters (rat and mouse), have suggested a role of the C-terminal fragment in the targeting of the symporter to the plasma membrane, and/or in its stabilisation [25–27]. A specific focus on this domain should therefore bring precious information concerning NIS post-translational regulation.

In our laboratories we have established eukaryotic cell lines stably-expressing various hNIS recombinant proteins at a relatively high level (around one percent of the total membrane protein), and developed a purification protocol based on immobilized metal affinity chromatography (IMAC) and immuno-affinity chromatography using in-house antibodies. This allowed us to purify, for the first time, milligram quantities of this human transporter. Thus purified, the protein exists in different structural forms, which were further characterised and analysed by size exclusion chromatography (SEC) and light scattering (LS) spectroscopy, in order to determine the hNIS oligomeric state. Besides, we have also characterised in detail a C-terminal fragment of NIS that co-purifies with the full-length protein expressed in HEK 293 cells. This fragment was found in physiological situations and in all cell types expressing NIS that we tested. Edman sequencing allowed us to define its first amino acid residues, showing that it is constituted of the 131 last amino acid residues of the transporter, and therefore of the last transmembrane helix. The possible origin of the fragment was investigated and is discussed. Expression of either the N-terminal truncated domain (fragment [1–512]) or the C-terminal domain (fragment [512–643]) alone, as well as co-expression of the two fragments, was performed. In each case the proteins were characterised by immunofluorescence and cell surface biotinylation experiments in order to investigate their localisation, and by iodide uptake measurements to study their functional activity.

The overall analyses revealed important features and highlighted several interactions which may contribute to the post-translational mechanisms that finely tune iodide accumulation through hNIS regulation.

2. Materials and methods

2.1. Materials

All chemicals were purchased from Sigma-Aldrich, unless otherwise specified. Cell culture media and reagents were obtained from Gibco or Invitrogen. BCA was obtained from Pierce, LDS loading buffer and electrophoresis MOPS buffer were obtained from Invitrogen; DDM (reference D310) was purchased from Anatrace and C12E8 (reference 74,680) from Fluka. TetraHis antibody was purchased from Qiagen, the anti β-tubulin monoclonal antibody (clone D66) from Sigma-Aldrich, the anti pan cadherin from Anaspec (Fremont, CA, USA), and ECL plus from Amersham.

2.2. Construction of expression vectors and establishment of recombinant cell lines

Several human sodium/iodide symporter variants were sought with i) no Tag (hNIS), ii) a 6-histine tag at the C-terminus (hNIScH), iii) a FLAG tag (MDYKDDDDK) at the N-terminus and a 6-histine tag at the C-terminus (hNISnFcH), and iv) a FLAG tag and a 6-histine tag at the C-terminus (hNIScFH). For this purpose, hNIS gene was amplified with the appropriate primers, using a FL*-hNIS/pcDNA3 template (kindly provided by S. M. Jhiang, Ohio State University, USA). The PCR products were cloned into pcDNA5-FRT (Invitrogen) by restriction digest and the absence of unwanted mutations was confirmed by DNA sequencing.

hNISMDAE (variant with methionine 512 and aspartic 513 residues replaced by alanine and glutamic residues, respectively) was generated using a protocol based on the QuickChange™ site-directed mutagenesis protocol of Stratagene. After amplification of the hNIScH plasmid with the primers 5′-GCCCCCAGCTCAGGAGCG-GAAGCCAGCCGACCCGCCTTAGC-3′ and 5′-GGGTCGGCTGGCTTCCGCT CCTGAGCTGGGGGCCCTGCTGG-3′, the reaction mix was digested with *Dpn*I before transformation into *Escherichia coli*.

hNIS 1–512 (hNIS fragment [1–512] with a 6-histidine tag at the C-terminus) was constructed using PCR with the following primers: 5′-CTATAGGCTAGCGCCACCATGGAGGCCGTGGAGACCGGG-3′ and 5′-TAA CGTGAATTCTTAATGGTGATGGTGATGATGCATTCCTGAGCTGGG GGCCCTGC-3′. The product was digested with *Nhe*I and *Eco*RI and cloned into the MCS1 of the pIRES vector (BD Biosciences Clontech). hNIS 512–643 (hNIS fragment [512–643]) and NIS2P (hNIS fragments [1–512]-6histidine tag and hNIS fragment [512–643]) were constructed using PCR with the following primers: 5′-GGATCCTCTAGAG CCACCATGGACGCCAGCCGACCCGCC-3′ and 5′-AGGGATGCGGCCGCT-CAGAGGTTTGTCTCCTGCTGGTC-3′. The products were digested with *Xba*I and *Not*I and cloned into the MCS2 of the pIRES vector and hNIS 1–512, respectively.

Stable cell lines expressing NIS were generated from Flp-In™ 293 (Invitrogen) according to the supplier's protocol. HEK 293-T cells transitorily expressing NIS were transfected with FuGene (Roche) with an efficiency of approximately 60–70%.

2.3. Cell culture and protein expression

For culture in wells, HEK 293 cells were grown in Dulbecco's modified Eagle's medium (DMEM with glutamine) supplemented with 10% foetal calf serum, penicillin (100 units/ml) and streptamycin (100 μg/ml) until approximately 60% cell-confluence was reached, as detailed in [27]. For protein expression studies, cells were grown in DMEM supplemented with 10% foetal calf serum, penicillin/streptamycin mix as above (Gibco), and hygromycin (200 μg/ml) until transfer to the bioreactor SGI (Setric genie Industriel) for 3 l cultures or Biostat B1 (B. Braun) for 10 l cultures. Inoculation was performed at a cell density of 250,000 cells/ml. The culture was usually stopped after 6 days, corresponding to a plateau in cell density and the beginning of a decrease in cell viability. Culture conditions were pH 7.3, 30% PO_2, 37 °C and 50 rpm stirring. The time-period from frozen cell stock to cell-collection was generally around 4 weeks, at which point cells were washed in phosphate saline buffer and frozen at −80 °C until further use.

2.4. Iodide uptake

Iodide uptake in whole cells was performed according to [27] with 30 μM NaI and ^{125}I. Measurements were made after 5, 15, 30 and 60 min. The radioactivity was measured using a gamma counter (Packard) and for each set of experiments the value was normalized to the counts obtained for hNIS at 60 min. For transiently transfected cells, the same batch of HEK 293 cells was used for all the constructs, and the uptake was performed 48 h after transfection. For stable cell lines, values were normalized to the total amount of protein per well.

2.5. Antibodies against NIS

NIS 22R and 23R are in house rat monoclonal antibodies, raised against hNIS 625–640 peptide. NIS 39 S is an in-house mouse monoclonal antibody raised against purified hNIS and targeting a region located at the C-terminal intracellular domain of the protein (between amino acid residues 580 and 600). This antibody does not cross-react with a rat or a mouse NIS. Ab25 anti-mNIS is an affinity-purified rabbit polyclonal antibody raised against two peptides of mouse NIS [27]. This antibody cross-reacts with rat NIS.

2.6. Immuno-fluorescence experiments

Immunofluorescence labelling was performed according to [27] using NIS 39 S or TetraHis, diluted in PBS, 0.1% BSA at 14.6 μg/ml or 0.1 μg/ml, respectively.

2.7. SDS-PAGE, immunoblot analyses and deglycosylation experiments

Western blot analyses, comparing the effect of different tags on NIS protein expression, or the different variants, were performed according to [27] on total cell extract using a 10% or 15% SDS-PAGE, a RIPA lysing buffer (10 mM tris-HCl, 150 mM NaCl, 1 mM EDTA, 1% Triton X-100, +/−0.1% SDS, protease inhibitors Complete (Roche)), a loading buffer containing 2% SDS, 100 mM DTT plus 0.2% beta-mercaptoethanol, a PVDF membrane, I-Block (Tropix) as a blocking agent. The antibodies were diluted in PBS, 0.1% BSA and the Amersham ECL plus enhanced chemiluminescence detection system or the Pierce SuperSignal West Pico chemiluminescent substrate system were used for signal detection.

Western blot analyses concerning the purification were performed on a Phast system (GE Healthcare) and detection was performed by an overnight incubation with the antibodies, and using the anti-mouse or anti-rat Elite kits from Vectastain. For staining, the colorimetric DAB kit (Vectastain) was used. SDS-PAGE gels for silver nitrate staining were obtained from Invitrogen (Novex NuPAGE, 4–12% Bis–tris) and run in MOPS/SDS buffer. For these experiments, samples were prepared in Invitrogen LDS buffer containing 0% or 5% beta-mercaptoethanol.

Deglycosylation experiments were performed on purified hNIS protein using the N-glycosidase F kit from Roche, according to the supplier's instructions.

2.8. Cell surface biotinylation

Cell surface biotinylation experiments were performed according to [27]. 48 h after transfection, cells were washed twice with biotinylation washing buffer (9.6 mM Na_2HPO_4, 15 mM KH_2PO_4, 0.1 mM $CaCl_2$, 1 mM $MgCl_2$, 138 mM NaCl, 2.7 mM KCl). They were then incubated for 30 min at 4 °C in the same buffer supplemented with 1 mg/ml sulfo-NHS-SS-biotin (Pierce). Remaining free Sulfo-NHS-SS-biotin was removed by three washes with ice-cold biotinylation washing buffer containing 100 mM glycine. The cells were then lysed for 15 min at 4 °C in lysis buffer (0.1% SDS, 1% triton X-100, 150 mM NaCl, 1 mM EDTA, 100 mM tris-HCl pH 7.5, 1 μg/ml aprotinin and 1 μg/ml leupeptin). Lysates were centrifuged for 15 min at 14,000 g and loaded on streptavidin agarose beads (Immunopure Immobilized Streptavidin, Pierce). After 1 h incubation at room temperature, the suspension was centrifuged for 5 min at 14,000 g and the pellet was washed three times in the lysis buffer. Bound proteins were recovered by the addition of elution buffer (60 mM tris pH 6.8, 2% SDS, 10% Glycerol, 5% β-mercaptoethanol, 0.002% bromophenol blue), and analysed by western blot.

2.9. Membrane vesicle preparation and protein purification

Cells were thawed on ice, suspended in 10 mM HEPES buffer, pH 7.5 containing 250 mM sucrose, 1 mM EDTA and the inhibitor cocktail Complete (Roche-Applied-Science) (10 ml buffer per g cells (weight wet)), and disrupted using a cell disrupter (Cell D, Constant system) at a pressure of 0.3 kbar. After breakage, the lysate was centrifuged at 1000 g for 10 min. The supernatant was then centrifuged at 10,000 g for 10 min and finally at 370,000 g for 1 hour. The pellet was suspended in the same buffer, to a protein concentration of 20 to 30 mg/ml, as measured by the BCA assay. Membrane vesicles were aliquoted, frozen in liquid nitrogen, and stored at −80 °C until further use.

Membrane vesicles were rapidly thawed at 37 °C and diluted in 20 mM HEPES pH 7.5 buffer containing 0.5 M NaCl, 10% glycerol, 10 mM imidazole and protease inhibitors (Complete EDTA free, Roche-Applied-Science). After centrifugation for 1 h at 370,000 g and 4 °C, the pellet was suspended in the same buffer to a concentration of 2.2 mg/ml. Dodecylmaltoside (DDM) was then added dropwise from a 10% (w/v) stock solution to a final concentration of 1%, and the solution was maintained under magnetic stirring for 30 min at 4 °C. Unsolubilised material was removed by a 1 h centrifugation at 370,000 g at 4 °C, and the supernatant was loaded for IMAC using an AKTA FPLC, onto a 5 ml HiTrap Chelating HP (GE Healthcare) previously loaded with nickel ion, and equilibrated with a 20 mM HEPES pH 7.5 buffer containing 0.5 M NaCl, 10 mM imidazole, 0.05% DDM, plus protease inhibitors. After binding of the protein, the column was washed with the same buffer containing 40 mM imidazole and the protein eluted at 250 mM imidazole. Only a small proportion of the transporter eluted at 450 mM imidazole. For immuno-affinity purification, the NIS22R antibody was coupled to a CNBr activated Sepharose 4FF matrix with an antibody/gel ratio of 2 mg/ml. The 250 mM imidazole fraction (10 ml) was diluted by a factor of three in 20 mM HEPES buffer, pH 7.5 containing 150 mM NaCl and 0.05% DDM, and incubated overnight with 10 ml of the antibody coupled gel. The gel was then packed in a column and washed with the same buffer. Protein elution was performed with citrate buffer pH 3.5 followed by HCl Glycine buffer pH 2.5. The fractions were immediately neutralised with 1 M tris buffer, pH 8.

At each step after solubilisation, the protein concentration in the fraction was estimated by UV absorption measurement at 280 nm against the appropriate buffer. In the case of imidazole-

containing buffers, the absorption at 305 nm was used to correct for the real contribution of this salt in the fraction. The value of 1.4 OD for a 1 g/l solution and a 1 cm path length cuvette was used throughout the purification and corresponds to the theoretical value for a 0.1% in mass hNIScH solution, as calculated according to Gill and von Hippel [28].

For experiments with Triton or C12E8, the purification protocol and buffers were the same as described above except that, for solubilisation, the 1% DDM was replaced by 1% TX-100 or 1% C12E8, and the 0.05% DDM was replaced in the subsequent buffers by 0.1% TX-100 or 0.025% C12E8 (around five times the critical micelle concentration (CMC) in all cases).

2.10. Size exclusion chromatography and light scattering analyses

SEC analyses were performed using an Agilent HPLC and a TSK G4000 SWXL column from Tosohaas. The buffer was a 50 mM phosphate buffer, pH 6.7, 150 mM NaCl, 0.05% DDM, with a flow rate of 0.5 ml/min. For LS analyses, the buffer was filtered at 0.1 μm instead of 0.22 μm. Samples were also concentrated on microcon YM-100 (Millipore) before injection (around 100 μl). LS analyses were performed with an online detection chain comprising the Agilent HPLC with its UV detection cell, the miniDAWN Tristar multi-angle LS detector and the Optilab rEX differential refractometer from Wyatt technologies. Results were analysed with the ASTRA program (Version 5.3.1.8) and the specific module protein conjugate. We used values of 0.185 and 0.133 ml g^{-1} for the protein and DDM dn/dc (specific refractive index increment), respectively, and of 1400 and 1.4 ml g^{-1} cm^{-1} for UV extinction coefficients [29].

2.11. Protein sequencing

After purification, and concentration on a microcon YM-30, 120 μg of the immuno-affinity fraction (eluted at pH 3.5) of hNIScH were injected onto a TSK G2000 SWXL column for size exclusion chromatography (phosphate buffer, 0.05% DDM, 1 mM DTT). The peak corresponding to the free C-terminal fragment was collected, the protein was concentrated on a microcon YM-3 and, after incubation with LDS (lauryl dodecyl sulphate) buffer, was loaded onto a 12% bis–tris SDS-PAGE (Novex, NuPAGE Invitrogen) in five wells. After electrophoresis in MES (4-morpholineethanesulfonic acid) buffer, the proteins were transferred onto a PVDF membrane (Immobilon PSQ 0.22 μm) and the five bands were excised after staining with Coomassie® R-250. The membrane fragments were analysed by Edman sequencing on a Procise 49X HT protein sequencer (Applied Biosystems) connected to a RP-HPLC for the identification of the step-wise released phenylthiohydantoin amino acid derivatives. A second sequencing experiment was performed in similar conditions, except that the size exclusion chromatography column was a TSK G3000 SWXL.

3. Results

3.1. Expression of hNIS in HEK 293 cells and comparison of the effect of various tags

hNIS cDNA was expressed in HEK 293 cells. To facilitate purification, tags were added to the protein (6-histidine and/or Flag tags) at different positions (C and N-terminus), and the effects of these additions were first analysed by measuring iodide uptake in transiently and stably transfected cells. The data presented in Fig. 1A show that the addition of a Flag tag at the N-terminal extremity and a 6-histidine tag at the C-terminal end of hNIS protein (hNISnFcH) resulted in a very significant loss of activity compared with wild-type, hNIScH or hNIScFH (i.e., 40% +/−2% of hNIS iodide uptake for hNISnFcH stable cell line after 1 h).

Western blot analyses also indicated that the construct hNISnFcH generated much less NIS protein and that the protein produced was less-glycosylated (Fig. 1B). In addition, hNIS appeared to be less aggregated in stable cell lines than in transiently transfected cells.

Immunocytochemistry (Fig. 1C) revealed that the fusion of a Flag tag at the N-terminus of the transporter resulted in an increased intracellular form of the protein compared to the other modifications or to the wild type. For stable cell lines, the results presented in Fig. 1 were obtained using several independent clones.

Overall, these data showed that the construct hNISnFcH was not appropriate for our study. In the rest of the report, the stable cell line generated with the hNIS cDNA encoding for a 6 histidine tag at the C-terminus of hNIS (hNIScH) was used.

3.2. hNIS expression and purification

For purification of NIS protein, hNIScH-expressing cells were grown in suspension. The yield per litre in optimal conditions was 15 g of cells (wet weight) yielding vesicles containing about 250 mg total membrane proteins. These membrane vesicles were solubilised with DDM with a yield of approximately 70% for hNIS protein, as estimated by western blot (Table 1). IMAC with nickel ion was used to capture the hNIS protein fraction. Loading with 10 mM imidazole and washing with 40 mM imidazole allowed the elimination of more than 97% of the contaminating membrane proteins, without any detectable hNIS loss in the flow-through or washes. The protein was eluted with 250 mM imidazole. At this point, hNIS was still highly contaminated by other proteins (Fig. 2A, first lane). This first step of chromatography was, therefore, followed by an immuno-affinity chromatography with an in-house antibody NIS22R and an acidic elution at pH 3.5, followed by an immediate neutralisation. A fraction of the protein eluted only at lower pH (2.5) and was not used any further as its characterisation showed more-aggregated forms. As indicated in Table 1, and based on five such purifications, around 1.2 mg of hNIS per 250 mg of membrane proteins was obtained in the pH 3.5 fraction. Direct immuno-affinity purification reduced the yield.

3.3. Identification of the different hNIS species present

Western blot analyses were performed with antibodies recognising different epitopes on hNIS (NIS23R and NIS39S) and the 6-histidine tag (TetraHis antibody) (Fig. 2A, lane 3, 4 and 5). The results highlighted bands that were similar to those stained with silver nitrate (Fig. 2A, lane 2), suggesting that the proteins in the elution fractions were merely different forms of hNIS. The migration pattern obtained by western blot was also identical to what was observed using membrane vesicles, indicating that these species already existed in the membranes and were not artefacts generated during the purification process (Fig. S1). To further characterise these different forms, deglycosylation was performed using N-glycosidase F. As shown in Fig. 2B, two of the main bands shifted towards a unique band of lower molecular weight, suggesting the co-existence of partially- and fully- (three glycosylations) glycosylated forms of the protein. This pattern of glycosylation is similar to observations made using thyroid tissue (healthy or not) [12] as well as transfected COS cells [10,30], and fits with the detailed analysis realized by Levy et al. on COS cells [10]. The higher molecular weight species, likely to correspond to a dimer, appeared also to be glycosylated. This was in sharp contrast to the 15 kDa band, which did not seem to be sensitive to N-glycosidase F. To confirm the identity of the proteins, the different bands on the SDS-PAGE gel stained with Coomassie blue were excised, subjected to in-gel trypsin digestion and analysed by mass spectrometry (MALDI-TOF). All analyses identified hNIS peptides and indicated that the 15 kDa band contained the C-terminal peptide, as suggested by western blot analyses (See Supplementary data S2).

To further the characterisation of this fragment, and as no peptide corresponding to a potential N-terminus could be detected by mass spectrometry (MALDI-TOF), we decided to perform Edman sequencing.

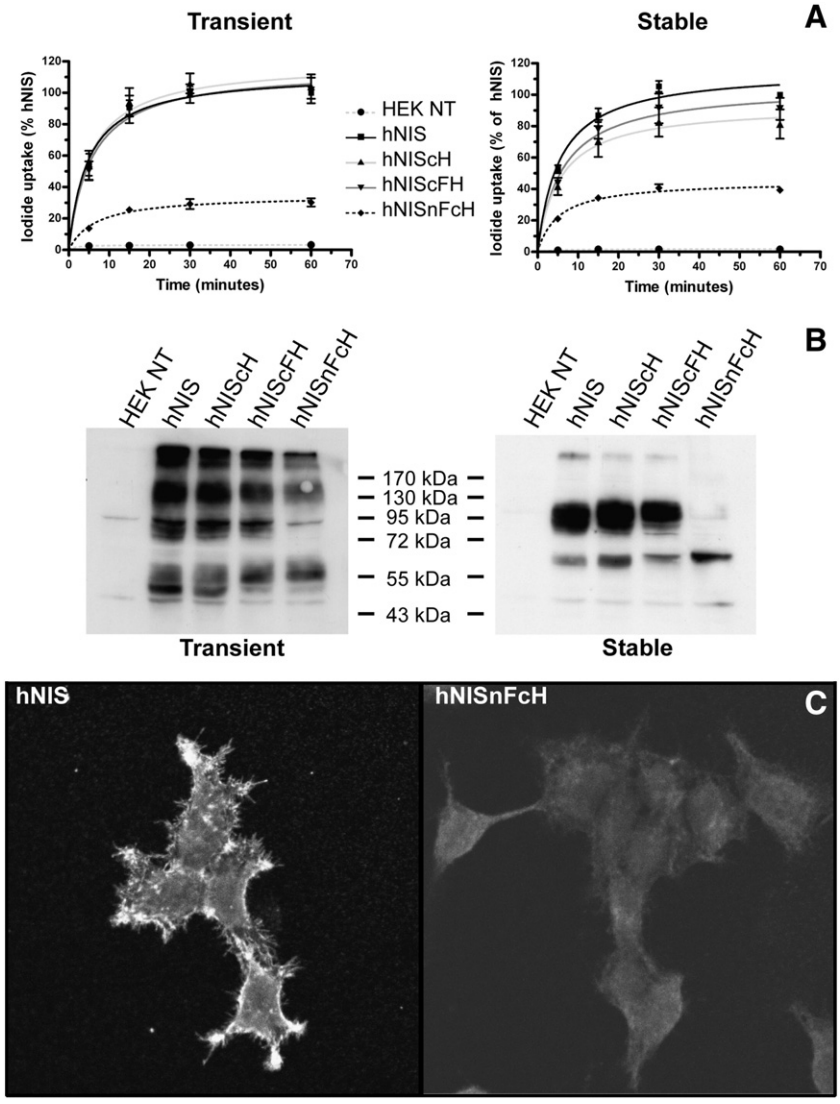

Fig. 1. Comparison of the effects of various tags. **(A)** iodide uptake in whole cells was performed with 30 μM NaI and various incubation times. After washing the cells, the intracellular content in ^{125}I was determined by gamma counting and, for each set of experiments, this value was normalized to the counts obtained for hNIS at 60 min (set to 100%). For stable cell lines, the values were previously standardized to the total amount of protein per well. The results plotted represent the average of four and three experiments for transiently (left) and stably (right) transfected cells, respectively, and with standard error bars. The curves are the corresponding hyperbolic fittings. HEK non-transfected cells: ●, light grey dotted fit; hNIS: ■, black fit; hNIScH: ▲, light grey fit; hNIScFH: ▼, dark grey fit; hNISnFcH: ♦, dark dotted fit **(B).** Western blot analyses were conducted on total extracts (with RIPA buffer) from transiently (left) and stably (right) transfected cells. 20 μg protein was loaded per well and separated on a 10% SDS gel. PVDF membranes were probed with NIS39S antibody diluted to 1.5 μg/ml and using ECL plus. Molecular weight markers are indicated and the immunoblots shown are representative of at least three independent experiments. **(C)** Immunolocalisation of hNIS protein variants with different tags was realized on stably transfected cell lines with the monoclonal antibody NIS39S. The images shown in the figure are representative of several independent transfections and multiple fields on the same slide. The confocal microscope used was a Pascal from Zeiss.

Table 1
hNIScH purification yields.

	Proteins in membrane vesicles[1]	Solubilized proteins[2]	Fraction after IMAC[3]	Fraction 1 after immuno-affinity (pH 3.5)	Fraction 2 after immuno-affinity (pH 2.5)
Yields	100%	69% ± 5.3	2.6% ± 0.3	0.46% ± 0.08	0.09% ± 0.03
	250 mg			1.15 ± 0.2 mg	

[1]The protein concentration in membrane vesicles was determined using the BCA assay. [2]At each step after solubilization, the protein concentration was estimated by UV absorption measurement at 280 nm and corrected for imidazole absorption when necessary. The theoretical value of 1.4 OD for a 1 g/l solution of hNIScH in a 1 cm path length cuvette was used throughout the purification. [3]The fraction after IMAC corresponds to the peak of proteins eluting at 250 mM imidazole. The figures in the table represent the average (and standard error) of five independent purifications. Membrane vesicles containing 250 mg protein are usually obtained for samples starting with about 3 l culture grown in the SGI bioreactor.

The first nine amino acid residues identified were DASRPALAD (See Supplementary data S3). This sequence matches perfectly the protein sequence derived from hNIS cDNA, starting at position D513. As this fragment was also revealed by the tetraHis antibody targeting the 6-histidine tag fused to the C-terminal end of the symporter, we concluded that this 15 kDa protein is, in fact, the last 131 amino acid residues of the NIS protein. Its theoretical molecular weight is 14,067 Da (15,340 Da with the 6-histidine tag) and it contains the last predicted transmembrane helix. From the primary structure, no glycosylation is indeed expected.

3.4. Polydispersity of the purified transporter

Considering the high degree of heterogeneity of hNIS, illustrated by the pattern of bands in SDS gels, SEC was used to achieve a better characterisation and, perhaps, to purify hNIS to a higher degree of homogeneity. Fig. 3A shows a typical elution profile with UV

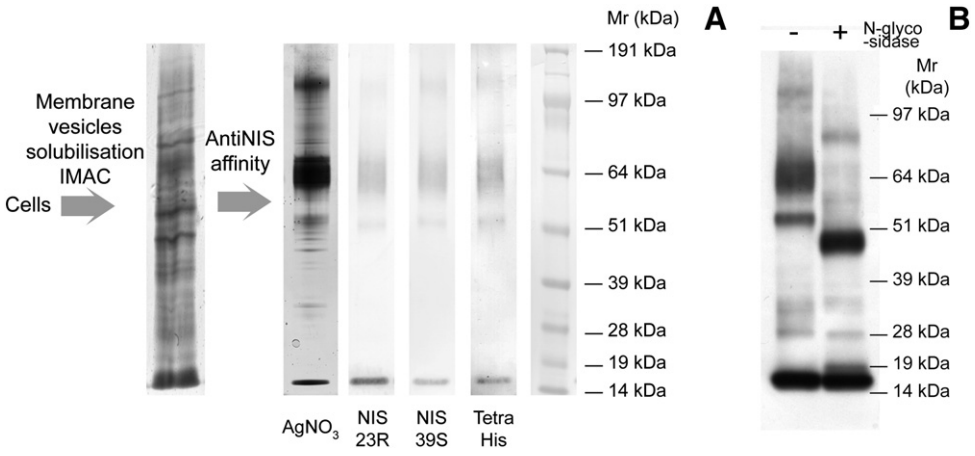

Fig. 2. Analysis of the fractions during hNIScH purification and characterisation of the glycosylated species. **(A)** The purification fractions after IMAC and after immuno-affinity chromatography with the antibody NIS22R were analysed on a 4–12% Bis–tris gradient gel run in MOPS buffer (Invitrogen). Lanes 1 and 2 are stained with silver nitrate. After transfer onto a PVDF membrane, lane 3, 4 and 5 are probed with NIS23R and NIS39S (two antibodies recognising different epitopes on hNIS) and the TetraHis antibody (Qiagen), respectively. Lane 6 corresponds to the See Blue plus 2 molecular weight marker (Invitrogen). **(B)** The deglycosylation experiments were performed on purified hNIScH protein, using N-Glycosidase F according to the supplier's instructions (Roche). The analysis was performed on a 4–12% Bis–tris gradient gel run in MOPS/SDS buffer (Invitrogen). The proteins were transferred onto a PVDF membrane which was probed with the TetraHis antibody (Qiagen). Molecular weights are indicated in kDa.

monitoring and the western blot associated with each fraction. The protein does not elute as a single monodisperse peak, indicating that purified hNIS is present in various oligomeric states. To verify that this heterogeneity was not associated with the purification process, and especially with the acidic elution, the same analyses were performed just after solubilisation (and also after IMAC). The UV profile could not be used due to the contribution of the other proteins, however the western blot pattern was similar with hNIS protein eluting in some high molecular weight fractions (See Fig. S4). Two other detergents (Triton X-100 (TX-100) and octaethylene glycol monododecyl ether (C12E8)) were also used to solubilise and purify hNIS. SDS gel and western blot analyses revealed a pattern comparable to the one obtained with DDM, with similar levels of monomer, dimer and higher forms (See Fig. S5).

3.5. Molecular weight determination of the different forms of hNIS by SEC-LS/UV/RI

The major peak of hNIS eluted during SEC at a MW of approximately 200–250 kDa, according to soluble MW standards. This was rather high for a membrane protein of approximately 70 kDa, even with its detergent crown. We therefore coupled SEC to an online LS analysis system (Wyatt technologies) to determine more precisely the molecular assemblies present in the purified sample

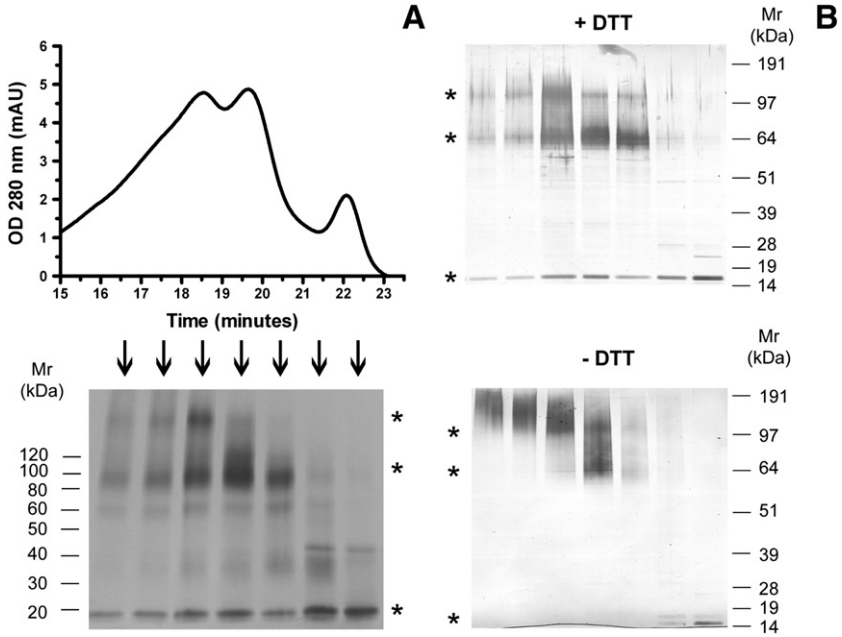

Fig. 3. Size exclusion chromatography analysis of purified hNIScH and effect of DTT. **(A)** A representative profile of size exclusion chromatography (SEC) on a TSK G4000 SWXL column of purified hNIScH monitored at 280 nm is shown in the upper panel. In the bottom panel, the western blot analysis of the associated fractions is shown. A Phast system (GE Healthcare) with 4–15% gradient gels, a transfer for 15 min on a 0.22 μm Immobilon PSQ membrane, and detection with the TetraHis antibody (Qiagen), the anti-mouse and the colorimetric DAB kits from Vectastain were used. Molecular weight marker: Magic Mark (Invitrogen) **(B)** Analysis of the effects of the reducing agent DTT on the SEC fractions of hNIScH was performed on 4–12% Bis–tris gradient gels run in MOPS/SDS buffer (Invitrogen), and representative gels stained with silver nitrate are shown. Molecular weight marker: See Blue Plus 2 (Invitrogen). Note that the proteins migrate with different apparent molecular weight in the two gel systems. For clarity, the three main bands have been pointed out on the side by a star.

under non-denaturing conditions. This global system, which includes a classical UV detector and a refractometer, in addition to the static LS module, allowed us to discriminate between the protein and detergent fractions. The amount of light scattered depends on the molecular weight, concentration, and specific refractive index increment (dn/dc) of the molecule. For soluble proteins, the concentration is determined by measuring the refractive index and using a dn/dc of 0.185 ml/g. Contrary to the extinction coefficient (ε), the dn/dc is almost amino acid-independent and, therefore, protein-independent. For membrane proteins, or proteins with sugars, the dn/dc of the complex or molecule is a linear combination of the dn/dc of the two entities based on their mass proportion in the assembly. It is therefore necessary to use a third detector (UV) and know the ε of the different species, as well as the dn/dc of the detergent alone [29,31]. One should also note that in the case of a glycosylated membrane protein, the three entities cannot be discriminated and the sugar moiety will be included in the detergent fraction as well as the tightly bounds lipids. The most effective column was the TSK G4000 SWXL but, despite its performance, the different oligomeric species could not be properly separated due, at least partially, to the detergent crown. LS analysis profiles, illustrated by one example in Fig. 4, indicated clearly the presence of several species with no molecular mass plateau. However, the peak with a summit at 19.2 in UV absorbance had a protein molecular weight close to that of a dimer and the one with a summit at 18.2 corresponded roughly to a tetramer. By using the postulate that tetramer and monomer never co-elute, we could calculate the proportion of each species that would sum to the experimentally calculated molecular weight determined by the ASTRA software in the range of the grey peak highlighted in Fig. 4A. The integration of these values gave the proportion of each oligomeric form. The results of five analyses on three different purifications are summarized in Table 2. As to the precise molecular mass of the small fragment, this could not be determined as the detergent micelle contributed too much to the diffusion signal. Another approach to extract the data from these overlapping species is to deconvolute the UV signal using Gaussian curves for each species. This was performed manually on one analysis (Fig. 4C) and here again, the integration allowed the determination of each species proportion, including the small C-terminal fragment, as DDM micelle interference with the UV signal is negligible. The results of this analysis on the 'full profile', or restricted to the selected grey peak range in Panel A, are shown in Table 2. A clear conclusion is that there is almost no monomer in purified hNIS fractions. The transporter is found mainly as dimers and tetramers. One should note at this point that part of the tetramer is not taken into account in the analyses on the grey peak range and, therefore, the monomer/dimer ratio is higher for these cases than for the analysis on the 'full profile'. According to these data, it also seems that the trimeric form, if it exists, is minor, but the analysis becomes less and less reliable in the higher molecular weight fractions due to a decreasing resolutive power of the size exclusion column in this molecular range.

3.6. NIS assembly is stabilised by disulfide bridges

The presence of the [513–643] fragment in SEC heavy fractions (Fig. 3A) suggested that it was associated with the full-length transporter, or with the remaining portion (N-terminal domain) of the transporter, if this exists as a self-entity. Experiments were, therefore, performed to test the effects of a reducing agent in the gel electrophoresis loading buffer, showing a clear difference in the SEC fractions pattern (Fig. 3B). Without DTT, the [513–643] fragment was no longer visible in the high molecular weight fractions, indicating that a disulfide bridge was implicated in the interaction. The proportion of dimer on the gel was also increased in the absence of reducing agent in the loading buffer, revealing that at least one disulfide bridge also contributed to the full-length transporter interactions and to the stabilisation of a dimeric species. However, adding a reducing agent before and/or during SEC was not sufficient to break the dimers (See Fig. S6).

3.7. The C-terminal fragment is present in NIS from various species and is not a product of internal translation

Even if it is difficult to estimate the proportions, the amount of the [513–643] fragment was clearly higher than that of the other faint intermediate bands distinguishable on silver nitrate-stained gels or western blot analyses, which most likely represented degradation products. To check that its presence was not an artefact of our expression system or that it was not limited to the human protein, the existence of such a C-terminal fragment was probed in thyroid cells and in other species. Western blot analyses were performed on samples obtained from human thyroid (biopsy from a patient with Graves' disease), from the rat thyroid cell line FRTL5 or from HEK 293 cells stably expressing mouse NIS. In all conditions, a strong 15 kDa band was visible when a NIS-specific antibody was used as the probe (Fig. 5). These data strongly suggest that the expression of the full-

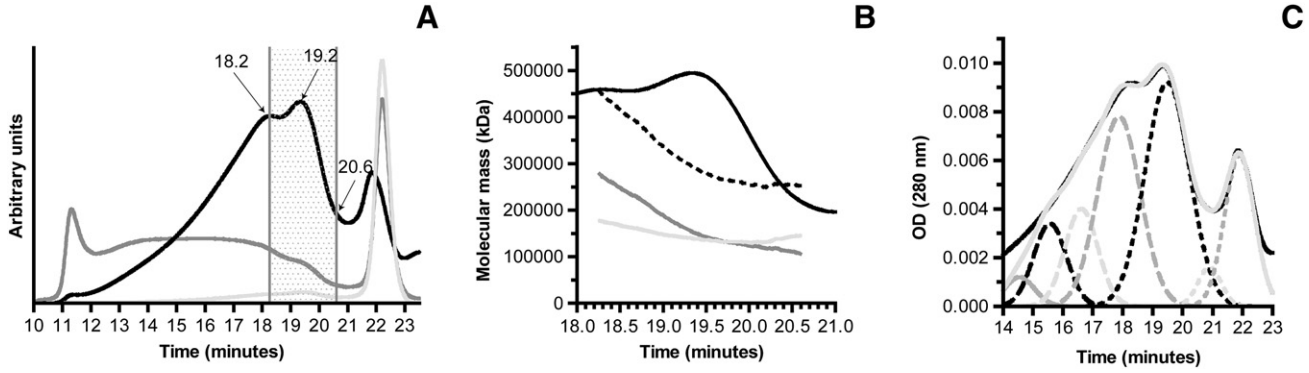

Fig. 4. Molecular mass analyses of hNIScH. Light scattering analysis was performed on the flow eluting from the TSK G4000 SWXL after injection of purified hNIScH. The results are representative of three different experiments. **(A)** Spectra corresponding to the UV signal at 280 nm, the Rayleigh ratio and the differential refractive index are shown in black, dark grey and light grey, respectively. The area between the elution times 18.26 and 20.6 is highlighted in grey (dots) and corresponds to the region analysed in more detail in Panel B. **(B)** The elution area highlighted in Panel A was analysed with the module protein conjugate from ASTRA software in order to determine the total molecular mass as well as the protein and detergent masses, and results are shown as black dashes, dark grey and light grey lines, respectively. The UV profile is shown in dark continuous line. **(C)** The UV experimental profile of hNIScH elution is shown in black. The curves corresponding to various Gaussian distribution associated with the theoretical elution of the different species are shown in dark grey, black long dashes, or light grey long dashes for HMW1, HMW2 and HMW3 respectively, and dark grey long dashes for the tetramer, black short dashes for the dimer, light grey short dashes for the monomer and dark grey short dashes for the C-terminal fragment. The light grey continuous line represents the sum of these multiple Gaussians curves and almost superimposes with the experimental signal. The areas below these curves were used to calculate the proportions of the different species, as stated in Table 2.

Table 2
Proportion of the various oligomeric species of purified hNIScH.

	HMW 1 species	HMW 2 species	HMW 3 species	Tetramer	Dimer	Monomer	C-terminus
ASTRA analysis 18.26–20.6 min range[1]				26.6% +/−3.3%	64.9% +/−4.2%	8.5% +/−6.5%	
UV deconvolution 14–23 min range[2]	2.5%	8.8%	10.4%	26.2%	32.4%	2.9%	14.5%
UV deconvolution 18.26–20.6 min range[3]				20.9%	77.9%	1.8%	

The proportion (mass percentage) of the various oligomeric species of purified hNIS was evaluated during size exclusion chromatography. [1]The analysis was performed on the elution range 18.26–20.6 min (highlighted by a grey dotted area in Fig. 4A), using the ASTRA software to evaluate the masses and followed by an integration for the different species. The results are the average of three different experiments. [2]The analyses were performed once on the elution range 14–23 min using a deconvolution of the UV signal as shown in Fig. 4C, followed by an integration, and attributing the different peaks to the species in concordance with light scattering results (tetramer, dimer or monomer). HMW1, HMW2 and HMW3 are three species of high molecular weight but ASTRA analysis does not allow a precise determination of their oligomeric nature. [3]The same analysis as described for B but on the elution range 18.26–20.6 min, in order to be closer to the ASTRA analysis.

length NIS protein is accompanied by the presence of a 15 kDa protein encompassing the C-terminal part of the protein.

However, as the amino acid residue preceding D513 in hNIS is a methionine residue conserved in the three species studied, we examined the possibility of an internal translation initiation site. A hNIS variant was generated to replace the methionine by an alanine residue. Fig. 6 shows that the 15 kDa protein band was still detectable in similar proportions. This result demonstrated that an internal initiation-of-translation is highly unlikely to explain the presence of this 15 kDa protein species. Altogether, these results suggest that the additional band observed is the result of cleavage of the full-length NIS protein.

3.8. Analysis of the potential role of this cleavage on NIS regulation

In order to gain insight into the potential role of the two domains, each fragment was transiently expressed in HEK 293 cells and the fragments were also co-expressed. The effects on NIS function, level of expression and localisation were analysed.

3.8.1. Iodide uptake in cells expressing the [1–512] fragment, the [512–643] fragment, or both fragments

First, iodide uptake was assessed in the resulting cells. Cells expressing the [1–512] and [512–643] fragments alone, or no NIS, accumulated after 1 h $3 \pm 0.5\%$, $4 \pm 0.6\%$ and $3.5 \pm 0.5\%$ of the iodide accumulated by the wild-type hNIS, respectively. Conversely, as shown in Fig. 7, around 9% ($8.7 \pm 0.9\%$) of the wild-type activity was recovered in cells expressing the two fragments (NIS2P). This activity of the split protein is low, but the difference is significant (P values inferior to 0.05 between NIS2P and hNIS 1–512, hNIS 512–643 or HEK not transfected for 15, 30 and 60 min).

3.8.2. Western blot analysis of cells expressing the [1–512] or [512–643] fragments, or both fragments

In order to analyse a potential stabilising role of co-expression, and to investigate if the low activity of the split protein was associated with a low expression level rather than with a poor intrinsic activity, western blot analyses of cells expressing the [1–512] or [512–643] fragments, or both fragments, were performed. As shown in Fig. 8, it was not possible to detect on western blot analyses, even with femto ECL, the presence of the [512–643] fragment expressed alone, whereas co-expression with the [1–512] fragment resulted in a faint, but clearly visible, band. As for the [1–512] truncated form, a faint and large band was visible when the protein was expressed alone or co-expressed with the [512–643] fragment. However, this expression represents only a small proportion of that of the full-length protein.

3.8.3. Protein localisation

Membrane proteins require correct targeting to be functional. To test the localisation of the different NIS fragments, immunocytochemistry was performed but no clear signal was observed.

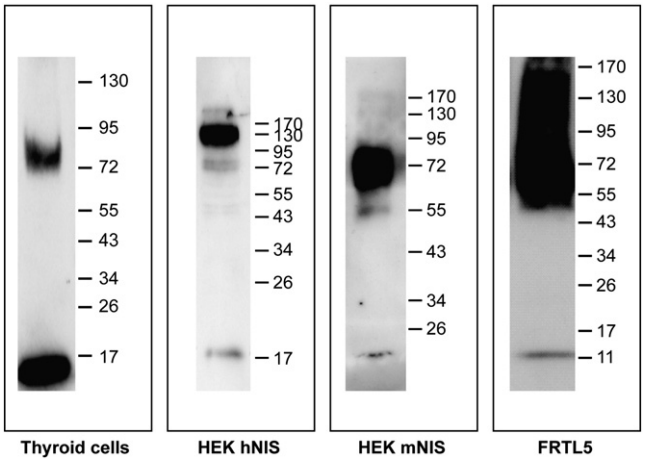

Fig. 5. Existence of a C-terminal fragment in various species. Western blot analyses were conducted on membrane vesicles from thyroid cells (patient with Graves' disease) (Lane 1), from HEK 293 cells stably expressing human (Lane 2) or mouse (Lane 3) NIS, and from the rat thyroid cell line FRTL5 (Lane 4). Proteins were separated on SDS gels and transferred onto PVDF membranes. These membranes were probed with NIS39S for hNIS (lane 1 and 2) and Ab 25 for mNIS and rNIS (lane 3 and 4).

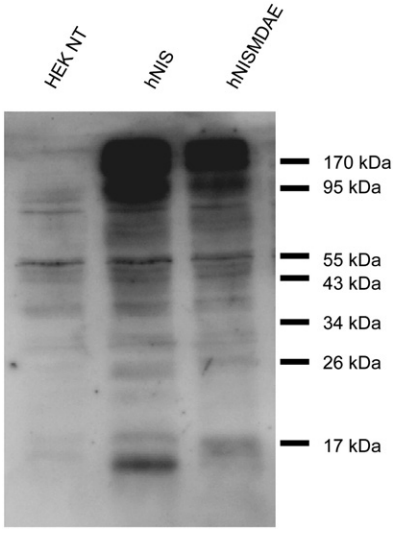

Fig. 6. Effect of the MDAE mutation on hNIS pattern. Western blot analyses were carried out using total extracts from transiently transfected cells. 40 μg protein were loaded per well and polypeptides were separated by electrophoresis through a 15% SDS gel. PVDF membranes were probed with NIS39S diluted at 1.5 μg/ml and using ECL plus. Molecular weight markers are indicated and the immunoblot shown is representative of three independent experiments. Lane 1 (HEK NT), non-transfected cells, Lane 2 (hNIS) cells transfected with the wild type hNIS and Lane 3 (hNISMDAE) cells transfected with the variant without the methionine.

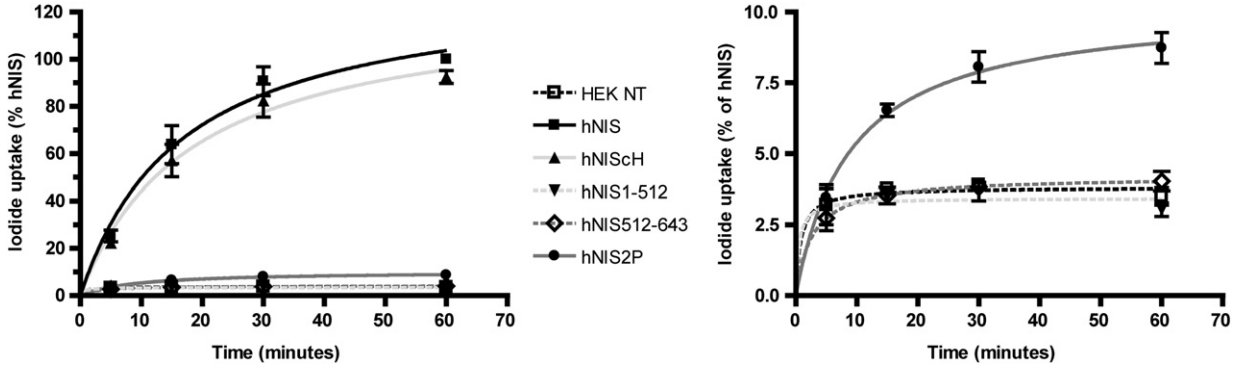

Fig. 7. Iodide uptake. Iodide uptake in transiently transfected, whole cells was performed with 30 μM NaI and various incubation times. After washing the cells, the intracellular content in ^{125}I was determined by gamma counting, and for each set of experiments this value was normalized to the counts obtained for hNIS at 60 min (set to 100%). The results plotted represent the average of three experiments with standard error bars with full scale on the left graph and a zoomed scale on the right graph to indicate hNIS2P activity more clearly. The curves are the corresponding hyperbolic fittings. HEK non-transfected cells □, black dotted fit; hNIS ■, black fit; hNIScH ▲, light grey fit; hNIS 1–512 ▼, light grey dotted fit; hNIS 512–643 ◊, dark grey dotted fit; hNIS2P ●, dark grey fit.

Expression of the [512–643] fragment alone produced a diffuse signal all over the cell. Its co-expression did not visibly affect the [1–512] fragment expression pattern (not shown). To determine more-precisely the influence of the [512–643] fragment on [1–512] fragment targeting to the plasma membrane, a more-quantitative method (biotinylation) was used. Fig. 9 shows that in both conditions a proportion of the [1–512] fragment could reach the plasma membrane. Quantification of the monomeric [1–512] fragment was performed by densitometry on three different western blot analyses (corresponding to two different biotinylation experiments) but no statistically significant stabilisation to the plasma membrane was observed upon co-expression of the [512–643] fragment.

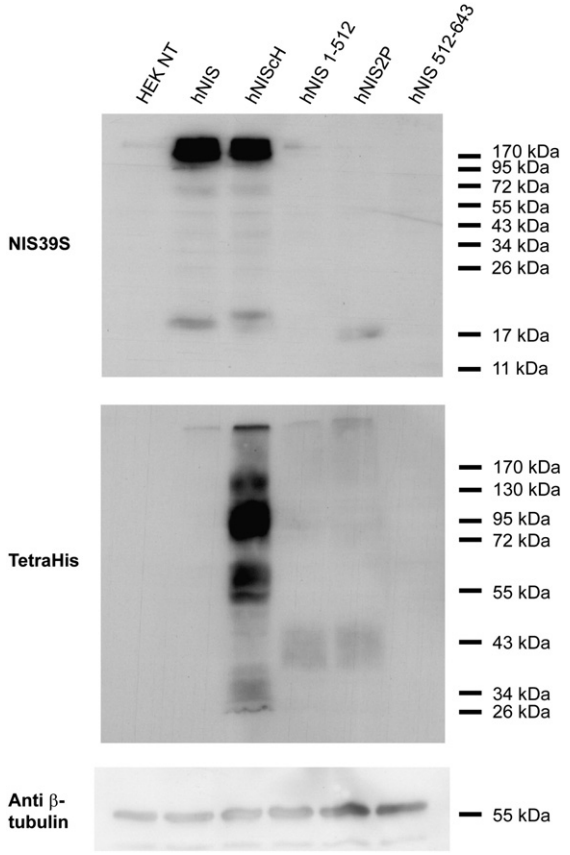

Fig. 8. Western blot analyses of hNIS 1–512, hNIS 512–643 and hNIS2P variants. Western blot analyses were conducted on total extracts from transiently transfected cells. 20 μg protein were loaded per well and polypeptides were separated by electrophoresis through a 15% (upper membrane) or 10% SDS gel (middle membrane). PVDF membranes were probed with NIS39S diluted at 1.5 μg/ml (upper membrane), TetraHis at 40 ng/ml (middle membrane) or anti β-tubulin at 1 μg/ml (lower membrane), and using ECL plus. The lower membrane corresponds to the middle membrane stripped and re-probed with the anti β-tubulin as a control. Molecular weight markers are indicated in kDa and the immunoblots shown are representative of three independent experiments.

4. Discussion

4.1. A Flag tag at the N-terminal extremity has negative effects on hNIS expression

In the present study, we generated various isogenic cell lines with several tags or tag positions, and observed important differences between them. Indeed, the cell line expressing the Flag tag at the N-terminal extremity (hNISnFcH) had less activity and produced less protein (especially in stable cell lines), and western blot analysis revealed that there was proportionally a lower degree of glycosylation. Images obtained by confocal microscopy showed, in addition, more intracellular sequestration of the transporter (Fig. 1C), suggesting a defect in the maturation process. Proteins produced from the construct hNISnFcH were purified and a proportion of them were noted to lack the Flag tag maybe due to a translation flaw or a proteolytic event. The two populations had a different pattern with more of the glycosylated form for the subpopulation without the Flag, confirming that the presence of the Flag interferes with the maturation process. This effect is not associated with the Flag tag sequence in itself, as when this tag is added to the C-terminus (hNIScFH cell line), no deleterious effects are observed. These results indicate that the presence of a Flag tag at the N-terminal extremity of NIS impairs its expression. Several studies have reported the tagging of NIS protein with an N-terminal Flag. In COS-7 cells, the presence of the N-terminal Flag does not affect iodide uptake as much as in HEK 293 cells [10,26]. However, western blot analysis showed that the pattern of bands differed greatly compared to the wild-type protein, with a preponderance of dimers and almost no monomer [10]. The absence of monomer has also been mentioned by Vadysirisack et al. [13], in HEK 293 cells. Therefore, the use of such a construct should be taken with great caution, especially when dealing with post-translational regulation.

4.2. hNIS can be expressed and purified in mg amounts

HEK 293 cells transfected with the hNIScH construct acquired the property of iodide accumulation, indicating that the protein was correctly folded in this cell line. Uptake assays were carried out after reconstitution into a lipidic environment to test the function of the purified protein, but these assays were not conclusive. However,

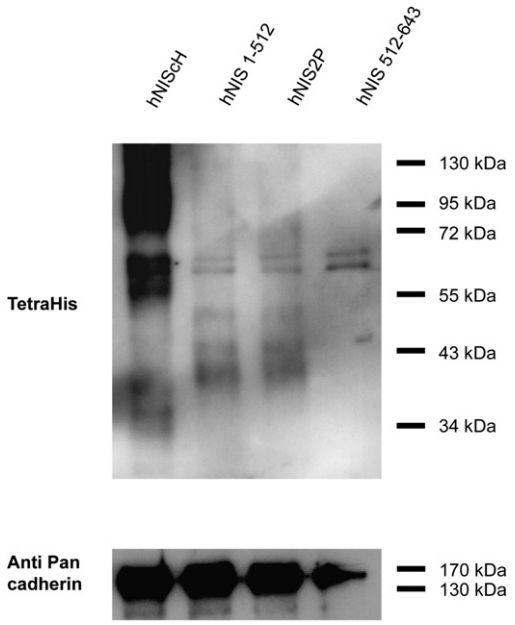

Fig. 9. Western blot analyses after cell surface protein biotinylation and immunoprecipitation. Western blot analyses were performed on samples obtained in cell surface biotinylation experiments as described in Experimental procedures. 5 µl aliquots were loaded per well and proteins were separated by electrophoresis through a 10% SDS gel. PVDF membranes were probed with the TetraHis antibody at 100 ng/ml and using ECL plus. The immunoblot shown is representative of four independent experiments.

preliminary experiments with Solid Supported Membranes (SSM) [32] have revealed some electrical signals in the presence of iodide and sodium, suggesting that the purified transporter is able, at least, to bind cooperatively these ions. In both cases, work is in progress to improve the quality of the proteoliposome reconstitution. Western blot analysis showed a heterogeneous pattern with monomer, oligomers and at least two levels of glycosylation, as well as a protein fragment. This pattern is unlikely to be an artefact as it is also observed in thyroid tissues. After immuno-affinity purification hNIS is recovered as a highly enriched fraction: on silver nitrate-stained SDS gels, the main bands all correspond to NIS molecules with very little, if any, contaminating proteins. Starting from 15 g cells, it was possible to obtain around 1.2 mg purified hNIS (Table 1). Moreover, after SEC, it was even possible, at the analytical level, to obtain a quasi homogeneous fraction (Fig. S7).

4.3. Characterisation of the hNIS C-terminal fragment

In this report, we have shown that the unexpected band observed during purification of hNIS expressed in HEK 293 cells, is also found in a cell line of thyroid origin as well as in biopsies of thyroid tissues. In the literature, this fragment can also be observed in other human tissues, such as kidney and breast [33,34], in the very few cases where reports show the low molecular range of western blots. This band has also been described by Castro et al. in COS7 cells expressing hNIS but, to date, no data are available regarding its sequence or properties [30].

Edman sequencing enabled us to determine the exact nature of this fragment. It corresponds to the C-terminal polypeptide of hNIS, starting from DASRPALAD and encompassing the last 131 amino acid residues (513–643 in hNIS).

One can note that the region encompassing amino acid residues 508 to 525 (and also the following transmembrane region) is well conserved between human, rat and mouse (PSSGMD-RPA-AD-FYA are identical amino-acids), and that a similar C-terminal fragment was detected in cells expressing the murine NIS.

In the human, rat and mouse, a methionine residue precedes the aspartic acid residue 513 in the full-length NIS protein. An internal translation initiation site of the C-terminal fragment could, thus, be envisaged. This phenomenon is, however, very rare in eukaryotes [35]. In addition, preceding an aspartic acid residue, the methionine should not have been processed and, therefore, should have been the first amino acid residue identified by Edman sequencing [36]. Analysis of putative alternative splicing events on the cloned human DNA sequence also did not predict such a fragment.

The finding that the human [512–643] fragment expressed alone was not detectable by western blot analyses (Fig. 8) constitutes an additional argument indicating that it is not expressed as a separate entity but is generated after production and insertion into the membrane of the full-length protein.

In addition, the fact that we could identify a unique amino acid at the N-terminal extremity suggests that the [513–643] fragment is not produced from a longer fragment shortened by an exoprotease, but rather is generated by a specific proteolytic cleavage of the polypeptide chain. We did not detect such a fragment when hNIS was expressed in *E. coli* (Fig. S8) suggesting that this mechanism may not be conserved in prokaryotes, or that the fragment is quickly degraded following its generation in bacteria.

According to topological models, the localisation of the cleavage site would imply that this phenomenon occurs intracellularly under the action of vesicular proteases, or extracellularly if the protein has reached the plasma membrane. In the latter case, ectoenzymes or secretory proteases could be involved. Such a specific proteolysis is not a rare phenomenon in channels and has already been described for the sodium phosphate co-transporter, for which it also occurs in an external loop [37–40].

However, a search in the literature and databases such as MEROPS (http://www.merops.sanger.ac.uk), did not identify the specific protease responsible for the proteolytic cleavage of NIS.

4.4. hNIS is present as different oligomeric forms but mostly as a dimer

Purified hNIS protein showed an electrophoretic pattern with dimers and higher oligomeric forms. We checked that this was not an aggregation due to DDM by using other non-ionic detergents: Triton X-100 and C12E8. Contrary to many studies, these protocols were carried out starting from membrane vesicle solubilisation, and led to the same heterogeneous pattern on western blots as DDM (Fig. S5). This pattern is, in fact, similar to previous analyses in our laboratory or in other laboratories in which thyroid tissues, cells or membrane vesicles are directly solubilised with SDS or LDS in the sample loading buffer [30,34]. Taken together, this suggests that this heterogeneity is not linked to the detergent itself but rather to the intrinsic state of hNIS in the membrane. Moreover, one can note that the western blot pattern for transiently transfected cells indicates more species with high oligomeric forms than for the stable cell lines, the patterns of which resemble the ones obtained for thyroid tissues. It is then reasonable to assume that the oligomeric state analysed in our HEK 293 stable cell line represents the real state in thyroid and is not associated with the saturation of the expression system or a defect in the maturation process.

Since this analysis was performed on denatured material, it was decided to apply an LS technique to determine absolute molecular weights of proteins in a more native state [31,41–43]. By using the molecular extinction coefficient calculated theoretically for NIS we were able to discriminate the fraction of detergent and protein in the molecular complexes analysed. This allowed us to confirm the existence in solution of different forms and to correlate them to the gel analyses. For hNIS, the main species encountered in solution is the dimeric form with, nevertheless, a high percentage of tetramer. For the predominant dimeric species, we found a mass ratio protein/detergent of around 1.1 and the proportion of detergent decreased to

a ratio protein/detergent of around 1.6 for the tetrameric form. In solution, the hNIS monomeric species represents less than 10% (Table 2).

This finding is in keeping with the data of Eskandri et al. on freeze fracture electron micrographs of NIS injected oocytes, which suggested the existence of the transporter as a multimeric form [1]. The structure of the *Vibrio parahaemolyticus* sodium/galactose symporter (vSGLT) has been solved recently [44]. Like NIS, this protein belongs to the sodium solute symporter family and has a sequence identity of 19% (58% similarity) with the iodide transporter. In the crystals, the protein assembles as a tightly packed dimer and this may indeed represent the structural unit of these family members.

4.5. Some interactions in NIS assemblies are stabilised by a disulfide bridge

The different electrophoretic patterns of hNIS in the presence or absence of a reducing agent in the loading buffer (Fig. 3B) clearly indicate that hNIS dimer assembly involves at least one disulfide bridge. However, the reducing agent alone, before and during SEC, is not able to dissociate dimers into monomers (See Fig. S6). This indicates that other strong interactions maintain the two subunits tightly associated together. The strength of these hydrophobic interactions is also highlighted by the fact that neither LDS nor SDS in the loading buffer can dissociate them, even in the presence of a reducing agent, as seen with the existence of dimers or multimers on SDS-PAGE gels. In addition, SDS-PAGE electrophoresis in reducing conditions of NIS dimeric species eluted in SEC are mostly dissociated into monomers, whereas for the fractions corresponding to the tetrameric form, a significant proportion migrates as dimers, strongly suggesting the existence of two distinct types of interaction (Fig.3). One could hypothesize that the tetrameric form may be, in fact, a dimer of dimers as is also assumed for sodium-dependent neurotransmitter transporters [23].

The different electrophoretic patterns of hNIS fragment in the presence or absence of a reducing agent in the loading buffer (Fig. 3B), as well as its presence in SEC heavy fractions (Fig. 3A) also clearly suggests that it is associated with the full-length transporter, or with the remaining portion (N-terminal domain) of the transporter, if this exists as a self-entity, and that a disulfide bridge is implicated in the interaction.

4.6. hNIS [1–512] and [512–643] fragments are in strong interaction and can reconstitute a functional transporter

The interactions between the C-terminal and N-terminal domains have been studied in more details. The co-expression of both fragments [1–512] and [512–643] in the same cells resulted in the restoration of iodide uptake, while each fragment expressed separately was devoid of activity (Fig. 7). The level of uptake achieved was only 9% of the wild-type NIS. These results suggest clearly that strong interactions exist between these two domains, and that they are able to reconstitute a functional protein. Considering the low level of expression achievable for both fragments, the reconstituted complex is highly active and a certain degree of structural flexibility is tolerated for iodide translocation in the last predicted external loop of hNIS.

This capability to reconstitute a functional transporter through the co-expression of protein fragments is not unique and has been described for membrane proteins such as Lac permease [45], the outer membrane protein OmpA [46], the voltage gated chloride channel CLC-1 [47], the cytochrome bc_1 complex [48], the sodium/glucose co-transporter [49], the sodium/calcium exchanger [50] or the type II sodium/phosphate co-transporter [51]. In the case of hNIS, we have demonstrated that the fragment [512–643] exists in cells at normal physiological conditions and, therefore, this observation has a higher degree of biological significance. These interactions are strong enough to be created without the help of a peptidic covalent link and rely mainly on hydrophobic contacts between helices.

Recently, the structure of the *Vibrio parahaemolyticus* sodium/galactose symporter (vSGLT) has been elucidated [44]. This protein belongs to the sodium solute symporter family and has a sequence identity of 19% (58% similarity) with NIS. In the crystals, the protein assembles as a tightly-packed dimer. Helix 13 is in proximity to TM7E, TM11 and TM12 in the same monomer and to TM3, TM11 and mainly TM13 in the other monomer. It is possible that similar interactions take place in NIS. In particular, the last transmembrane segment could be part of the dimerization interface. Castro et al. [30] clearly demonstrated the presence of a band around 30 kDa under non-reducing conditions, when analysing hNIS by western blot. This would suggest that the disulfide bridge implicated in the dimerization could involve two cysteine residues in this region but not one in the [513–643] fragment and one on the remaining part of NIS.

The knowledge that the hNIS [512–643] fragment expressed alone is not visible on western blot analyses, whereas when co-expressed with the hNIS [1–512] fragment a band is detected, implies that the two fragments are able to interact and that the [1–512] fragment stabilises the [512–643] fragment, which may be otherwise quickly degraded when expressed alone (Fig. 8).

4.7. The C-terminal domain is not absolutely required for NIS targeting

The C-terminal, cytosolic domain bears many potential regulatory sites including a PDZ protein binding site, di-leucine and di-acid motifs, and several phosphorylation sites; these sites are all potentially implicated in protein sorting, membrane or vesicle targeting and endocytosis. An attractive hypothesis would be that co-expression of the [512–643] fragment could bring the appropriate signal and/or protein–protein interactions required for the efficient targeting of the [1–512] fragment to the plasma membrane.

However, our biotinylation experiments contradict this hypothesis, as a proportion of the [1–512] fragment can reach the plasma membrane and co-expression of [1–512] and [512–643] does not significantly increase membrane targeting. These results imply that the C-terminal end of NIS is not absolutely required for membrane targeting and has no favourable effect at all as a [512–643] fragment.

This conclusion is discrepant with the conclusions drawn by Pohlenz et al. who reported that the mutant S515X, roughly similar to our hNIS [1–512] fragment, is not targeted to the plasma membrane but sequestered inside cells. The lack of absolute requirement of the PDZ protein binding site in the targeting was already suggested by the lack of effect, at least in non-polarized cells, of the addition of a 6-histidine tag in the C-terminal part of NIS (Fig.1, [27]). Indeed, this tag disrupts the PDZ recognition site but does not alter NIS membrane localisation. Considering all of the data available, we conclude that the putative regulatory sites present in the C-terminal part of NIS are probably not crucial, but rather act to finely-tune protein targeting or turnover.

In contrast, the presence of the C-terminal part of NIS appears to be very important for protein stability. When expressed as a truncated form, the level of expression of the N-terminal domain is low, suggesting instability. One could postulate that co-expressing the C-terminal domain would stabilise it. Indeed, the [512–643] fragment may contribute to the dimerization interface of the transporter and for some membrane proteins, such as in the sodium-dependent neurotransmitter symporter family, for example, the association in multimers is a prerequisite to pass the quality control mechanism in the endoplasmic reticulum and to reach the plasma membrane [23]. As discussed in the previous paragraph, the functionality of the split protein implicates proper interactions of the two domains and these interactions probably occur early in the maturation process. However, no stabilising effect was observed in our western blot analyses (Fig. 8),

suggesting a requirement for a peptidic bond between [1–512] and [512–643] for stabilisation.

4.8. Possible role of hNIS oligomeric assemblies and NIS cleavage

hNIS is present in cells as various oligomeric forms. It is acknowledged that the oligomeric state of some membrane proteins varies to regulate their function or control their interactions with other proteins. In the sodium-dependent neurotransmitter symporter family, for example, the association in multimer is a prerequisite to pass the quality control mechanism in the endoplasmic reticulum in order to reach the plasma membrane. We know that NIS is highly regulated at the post-translational level, but no precise data are available. In light of our results, a parallel can be drawn between NIS oligomeric states and what is known for neurotransmitter symporters that also co-transport sodium ion. A change in the equilibrium between the different forms of hNIS, including the rare monomeric form, could be a way to directly regulate iodide uptake by modulating protein targeting to the membrane. The role of oligomerisation in transport functionality is more controversial and the quaternary structure seems to play only a modest role in the transport cycle of bacterial transporters, for example [16]. However, the different interactions highlighted in this study could modify NIS interactions with partner proteins and hence its function or subcellular localisation.

Moreover, the physiological role of the [513–643] fragment is not yet understood but it is puzzling to find such an accumulation, even in healthy tissues and under physiological conditions.

According to the N-end rule pathway [52,53], and considering that this fragment starts with an aspartic acid residue, the [513–643] fragment should be ubiquitinylated and degraded. Its interaction with higher molecular forms of NIS (including disulfide bridge), or its orientation once in the membrane, may prevent this degradation from occurring. Due to the absence of an effective antibody recognising the [1–512] complementary fragment, and to the blurry pattern on the gel with the different oligomeric and glycosylated forms of NIS, it is technically difficult to determine whether the [1–512] fragment exists in physiological conditions and to assess the proportion of monomers which are, in fact, split monomers. The answer to these questions is crucial to the elucidation of the role of the [513–643] fragment. At this stage, several hypotheses can be put forward.

First, NIS cleavage may be associated with the regulation of protein turnover or stability at the membrane. It may, for example, trigger endocytosis and degradation of the N-terminal domain.

Second, if the fragment [513–643] accumulates as the N-terminal part of hNIS disappears, it may compete with monomers to prevent the formation of full-length dimers. The association of this fragment might, therefore, play an important role in hNIS quaternary structure regulation and, indirectly, could control the transporter function.

Third, the cleavage may have a direct effect on NIS catalytic function. Considering that expressing the NIS in two parts generates an active transporter, the role of the cleavage cannot be to inactivate hNIS function. Indeed, with a very low level of expression compared to that which can be achieved with the full-length protein (Fig. 9), and even if iodide uptake is not entirely proportional to the amount of hNIS protein in the plasma membrane, our data demonstrate that the split transporters are highly functional. However, a fine tuning of the activity cannot be excluded. For example, the total activity of inorganic phosphate transport is lower for the split II sodium/phosphate co-transporter [51]. However, this reduction is due to the lower level of protein expression and not to the electrogenic properties which are very similar in terms of substrate binding, pH and voltage dependency [51].

Alternatively, the cleavage might have a more specific functional role, as previously described for several channels. For example, the C-terminal domain of the calcium channel $Ca_V1.1$, is proteolytically processed, and interacts non-covalently with the remaining part of the channel and with the regulatory protein kinase (PKA) and A-kinase anchoring protein [37]. In the case of the sodium channel ENaC, processing occurs during the maturation with several proteases (furin, elastase, plasmin) to release inhibitory tracts [38]. In both cases, the protein is non functional in the absence of cleavage. Here for NIS, we know that a flexibility of the last external loop is tolerated for the function but, in fact, it may even be required. In this case, the cleavage would not have an inhibitory role, as is most often assumed, but rather an activating one.

Finally, in membrane protein fields, proteolytic events can occur to allow for the release of soluble domains, as in ectodomain shedding [54,55]. These fragments may then have separate functions. In our case, the cleaved fragment still has a membrane anchor and could, for example, link the cytoskeleton and scaffold complexes to the plasma membrane.

5. Conclusion

In conclusion, we present here an efficient expression system which allowed, for the first time, the production and purification of the human sodium/iodide symporter in mg amounts and in a form similar to what was observed in thyroid tissues. This enabled us to better characterise a C-terminal fragment of NIS encompassing the last putative helix of the transporter and existing as a separate entity, in humans, mice and rats. This [513–643] fragment is likely to be generated through a proteolytic cleavage of the full-length protein. We were also able to show that the protein exists mainly as a dimer stabilised by a disulfide bridge and that the [513–643] fragment is able to reconstitute with its [1–512] counterpart a functional symporter.

These results already represent an important step towards the understanding of the protein structural organization and provide clues as to the possible regulation of its function or localisation. In particular, the ability to separate (or highly enrich) the different oligomeric forms by SEC, in association with activity measurements, will enable us to determine which is the real functional unit.

Further experiments are required to understand the physiological significance of the [513–643] fragment, but the perspective of controlling this event will then give the opportunity to act on NIS activity and improve its clinical efficiency in the treatment of thyroid cancers and/or its use in radioiodine gene therapy.

Supplementary materials related to this article can be found online at doi:10.1016/j.bbamem.2010.08.013.

Acknowledgements

We would like to thank Yannick Delcuze and Julien Guglielmi for confocal microscopy, Isabelle Dany and Jean–Charles Gaillard for mass spectra analyses, and Philippe Guérin and Charles Marchetti for cell cultures. We are also grateful to Yves Brignon and Thierry Jouve for antibody production, and to Patrick Chang, Sabine Lindenthal and Georges Vassaux for their careful reading of our manuscript.

This work was supported by the CEA and by the program of Nuclear and Environmental Toxicology (France).

References

[1] S. Eskandari, D.D. Loo, G. Dai, O. Levy, E.M. Wright, N. Carrasco, Thyroid Na+/I- symporter. Mechanism, stoichiometry, and specificity, J. Biol. Chem. 272 (1997) 27230–27238.
[2] C. Riedel, O. Dohan, A. De la Vieja, C.S. Ginter, N. Carrasco, Journey of the iodide transporter NIS: from its molecular identification to its clinical role in cancer, Trends Biochem. Sci. 26 (2001) 490–496.
[3] O. Dohan, A. De la Vieja, V. Paroder, C. Riedel, M. Artani, M. Reed, C.S. Ginter, N. Carrasco, The sodium/iodide Symporter (NIS): characterization, regulation, and medical significance, Endocr. Rev. 24 (2003) 48–77.
[4] C. Spitzweg, J.C. Morris, The sodium iodide symporter: its pathophysiological and therapeutic implications, Clin. Endocrinol. 57 (2002) 559–574 (Oxf).

[5] A. De La Vieja, O. Dohan, O. Levy, N. Carrasco, Molecular analysis of the sodium/iodide symporter: impact on thyroid and extrathyroid pathophysiology, Physiol. Rev. 80 (2000) 1083–1105.
[6] G. Dai, O. Levy, N. Carrasco, Cloning and characterization of the thyroid iodide transporter, Nature 379 (1996) 458–460.
[7] P.A. Smanik, Q. Liu, T.L. Furminger, K. Ryu, S. Xing, E.L. Mazzaferri, S.M. Jhiang, Cloning of the human sodium lodide symporter, Biochem. Biophys. Res. Commun. 226 (1996) 339–345.
[8] B. Perron, A.M. Rodriguez, G. Leblanc, T. Pourcher, Cloning of the mouse sodium iodide symporter and its expression in the mammary gland and other tissues, J. Endocrinol. 170 (2001) 185–196.
[9] H. Jung, The sodium/substrate symporter family: structural and functional features, FEBS Lett. 529 (2002) 73–77.
[10] O. Levy, A. De la Vieja, C.S. Ginter, C. Riedel, G. Dai, N. Carrasco, N-linked glycosylation of the thyroid Na+/I- symporter (NIS). Implications for its secondary structure model, J. Biol. Chem. 273 (1998) 22657–22663.
[11] C. Riedel, O. Levy, N. Carrasco, Post-transcriptional regulation of the sodium/iodide symporter (NIS) by thyrotropin, J. Biol. Chem. 276 (2001) 21458–21463.
[12] S. Trouttet-Masson, S. Selmi-Ruby, F. Bernier-Valentin, V. Porra, N. Berger-Dutrieux, M. Decaussin, J.L. Peix, A. Perrin, C. Bournaud, J. Orgiazzi, F. Borson-Chazot, B. Franc, B. Rousset, Evidence for transcriptional and posttranscriptional alterations of the sodium/iodide symporter expression in hypofunctioning benign and malignant thyroid tumors, Am. J. Pathol. 165 (2004) 25–34.
[13] D.D. Vadysirisack, E.S. Chen, Z. Zhang, M.D. Tsai, G.D. Chang, S.M. Jhiang, Identification of in vivo phosphorylation sites and their functional significance in the sodium iodide symporter, J. Biol. Chem. 282 (2007) 36820–36828.
[14] D.D. Vadysirisack, A. Venkateswaran, Z. Zhang, S.M. Jhiang, MEK signaling modulates sodium iodide symporter at multiple levels and in a paradoxical manner, Endocr Relat Cancer 14 (2007) 421–432.
[15] T. Kogai, S. Sajid-Crockett, L.S. Newmarch, Y.Y. Liu, G.A. Brent, Phosphoinositide-3-kinase inhibition induces sodium/iodide symporter expression in rat thyroid cells and human papillary thyroid cancer cells, J. Endocrinol. 199 (2008) 243–252.
[16] L.M. Veenhoff, E.H. Heuberger, B. Poolman, Quaternary structure and function of transport proteins, Trends Biochem. Sci. 27 (2002) 242–249.
[17] R.R. Regeer, A. Nicke, D. Markovich, Quaternary structure and apical membrane sorting of the mammalian NaSi-1 sulfate transporter in renal cell lines, Int. J. Biochem. Cell Biol. 39 (2007) 2240–2251.
[18] M.N. Parvin, T. Gerelsaikhan, R.J. Turner, Regions in the cytosolic C-terminus of the secretory Na(+)-K(+)-2Cl(-) co-transporter NKCC1 are required for its homo-dimerization, Biochemistry 46 (2007) 9630–9637.
[19] L. Kao, P. Sassani, R. Azimov, A. Pushkin, N. Abuladze, J. Peti-Peterdi, W. Liu, D. Newman, I. Kurtz, Oligomeric structure and minimal functional unit of the electrogenic sodium bicarbonate co-transporter NBCe1-A, J. Biol. Chem. 283 (2008) 26782–26794.
[20] P. Fafournoux, J. Noel, J. Pouyssegur, Evidence that Na+/H+ exchanger isoforms NHE1 and NHE3 exist as stable dimers in membranes with a high degree of specificity for homodimers, J. Biol. Chem. 269 (1994) 2589–2596.
[21] I. Ubarretxena-Belandia, C.G. Tate, New insights into the structure and oligomeric state of the bacterial multidrug transporter EmrE: an unusual asymmetric homo-dimer, FEBS Lett. 564 (2004) 234–238.
[22] M. Ushimaru, Y. Fukushima, The dimeric form of Ca2 + -ATPase is involved in Ca2 + transport in the sarcoplasmic reticulum, Biochem. J. 414 (2008) 357–361.
[23] H.H. Sitte, H. Farhan, J.A. Javitch, Sodium-dependent neurotransmitter transporters: oligomerization as a determinant of transporter function and trafficking, Mol. Interv. 4 (2004) 38–47.
[24] G. Milligan, G protein-coupled receptor dimerisation: molecular basis and relevance to function, Biochim. Biophys. Acta 1768 (2007) 825–835.
[25] J. Pohlenz, L. Duprez, R.E. Weiss, G. Vassart, S. Refetoff, S. Costagliola, Failure of membrane targeting causes the functional defect of two mutant sodium iodide symporters, J. Clin. Endocrinol. Metab. 85 (2000) 2366–2369.
[26] Z. Zhang, Y.Y. Liu, S.M. Jhiang, Cell surface targeting accounts for the difference in iodide uptake activity between human Na+/I- symporter and rat Na+/I-symporter, J. Clin. Endocrinol. Metab. 90 (2005) 6131–6140.
[27] M. Dayem, C. Basquin, V. Navarro, P. Carrier, R. Marsault, P. Chang, S. Huc, E. Darrouzet, S. Lindenthal, T. Pourcher, Comparison of expressed human and mouse sodium/iodide symporters reveals differences in transport properties and subcellular localization, J. Endocrinol. 197 (2008) 95–109.
[28] S.C. Gill, P.H. von Hippel, Calculation of protein extinction coefficients from amino acid sequence data, Anal. Biochem. 182 (1989) 319–326.
[29] P. Strop, A.T. Brunger, Refractive index-based determination of detergent concentration and its application to the study of membrane proteins, Protein Sci. 14 (2005) 2207–2211.
[30] M.R. Castro, E.R. Bergert, T.G. Beito, P.C. Roche, S.C. Ziesmer, S.M. Jhiang, J.R. Goellner, J.C. Morris, Monoclonal antibodies against the human sodium iodide symporter: utility for immunocytochemistry of thyroid cancer, J. Endocrinol. 163 (1999) 495–504.
[31] Y. Hayashi, H. Matsui, T. Takagi, Membrane protein molecular weight determined by low-angle laser light-scattering photometry coupled with high-performance gel chromatography, Methods Enzymol. 172 (1989) 514–528.
[32] J. Pintschovius, K. Fendler, Charge translocation by the Na+/K+-ATPase investigated on solid supported membranes: rapid solution exchange with a new technique, Biophys. J. 76 (1999) 814–826.
[33] C. Spitzweg, C.M. Dutton, M.R. Castro, E.R. Bergert, J.R. Goellner, A.E. Heufelder, J.C. Morris, Expression of the sodium iodide symporter in human kidney, Kidney Int. 59 (2001) 1013–1023.
[34] I. Peyrottes, V. Navarro, A. Ondo-Mendez, D. Marcellin, L. Bellanger, R. Marsault, S. Lindenthal, F. Ettore, J. Darcourt, T. Pourcher, Immunoanalysis Indicates that the Sodium Iodide Symporter is not Overexpressed in Intracellular Compartments in Thyroid and Breast Cancers, Eur. J. Endocrinol. 160 (2009) 215–225.
[35] M. Kozak, Initiation of translation in prokaryotes and eukaryotes, Gene 234 (1999) 187–208.
[36] S. Huang, R.C. Elliott, P.S. Liu, R.K. Koduri, J.L. Weickmann, J.H. Lee, L.C. Blair, P. Ghosh-Dastidar, R.A. Bradshaw, K.M. Bryan, et al., Specificity of cotranslational amino-terminal processing of proteins in yeast, Biochemistry 26 (1987) 8242–8246.
[37] J.T. Hulme, K. Konoki, T.W. Lin, M.A. Gritsenko, D.G. Camp 2nd, D.J. Bigelow, W.A. Catterall, Sites of proteolytic processing and noncovalent association of the distal C-terminal domain of CaV1.1 channels in skeletal muscle, Proc. Natl Acad. Sci. USA 102 (2005) 5274–5279.
[38] C.J. Passero, G.M. Mueller, H. Rondon-Berrios, S.P. Tofovic, R.P. Hughey, T.R. Kleyman, Plasmin activates epithelial Na+channels by cleaving the gamma subunit, J. Biol. Chem. 283 (2008) 36586–36591.
[39] C.J. Boyer, Y. Xiao, A. Dugre, E. Vincent, M.C. Delisle, R. Beliveau, Phosphate deprivation induces overexpression of two proteins related to the rat renal phosphate co-transporter NaPi-2, Biochim. Biophys. Acta 1281 (1996) 117–123.
[40] Y. Xiao, C.J. Boyer, E. Vincent, A. Dugre, V. Vachon, M. Potier, R. Beliveau, Involvement of disulphide bonds in the renal sodium/phosphate co-transporter NaPi-2, Biochem. J. 323 (Pt 2) (1997) 401–408.
[41] Y. Wei, H. Li, D.Fu. Oligomeric, state of the Escherichia coli metal transporter YiiP, J. Biol. Chem. 279 (2004) 39251–39259.
[42] D. Yernool, O. Boudker, E. Folta-Stogniew, E. Gouaux, Trimeric subunit stoichiometry of the glutamate transporters from *Bacillus caldotenax* and *Bacillus stearothermophilus*, Biochemistry 42 (2003) 12981–12988.
[43] M. Aivaliotis, P. Samolis, E. Neofotistou, H. Remigy, A.K. Rizos, G. Tsiotis, Molecular size determination of a membrane protein in surfactants by light scattering, Biochim. Biophys. Acta 1615 (2003) 69–76.
[44] S. Faham, A. Watanabe, G.M. Besserer, D. Cascio, A. Specht, B.A. Hirayama, E.M. Wright, J. Abramson, The crystal structure of a sodium galactose transporter reveals mechanistic insights into Na+/sugar symport, Science 321 (2008) 810–814.
[45] E. Bibi, H.R. Kaback, In vivo expression of the lacY gene in two segments leads to functional lac permease, Proc. Natl Acad. Sci. USA 87 (1990) 4325–4329.
[46] R. Koebnik, In vivo membrane assembly of split variants of the E.coli outer membrane protein OmpA, EMBO J. 15 (1996) 3529–3537.
[47] T. Schmidt-Rose, T.J. Jentsch, Reconstitution of functional voltage-gated chloride channels from complementary fragments of CLC-1, J. Biol. Chem. 272 (1997) 20515–20521.
[48] A.S. Saribas, S. Mandaci, F. Daldal, An engineered cytochrome b6c1 complex with a split cytochrome b is able to support photosynthetic growth of Rhodobacter capsulatus, J. Bacteriol. 181 (1999) 5365–5372.
[49] Z. Xie, E. Turk, E.M. Wright, Characterization of the Vibrio parahaemolyticus Na+/Glucose co-transporter. A bacterial member of the sodium/glucose transporter (SGLT) family, J. Biol. Chem. 275 (2000) 25959–25964.
[50] M. Ottolia, S. John, Z. Qiu, K.D. Philipson, Split Na+-Ca2+ exchangers. Implications for function and expression, J. Biol. Chem. 276 (2001) 19603–19609.
[51] C. Ehnes, I.C. Forster, K. Kohler, J. Biber, H. Murer, Functional studies on a split type II Na/P(i)-co-transporter, J. Membr. Biol. 188 (2002) 227–236.
[52] A. Bachmair, D. Finley, A. Varshavsky, In vivo half-life of a protein is a function of its amino-terminal residue, Science 234 (1986) 179–186.
[53] T. Tasaki, Y.T. Kwon, The mammalian N-end rule pathway: new insights into its components and physiological roles, Trends Biochem. Sci. 32 (2007) 520–528.
[54] M.M. Hoefer, H. Illges, Ectodomain shedding and generation of two carboxy-terminal fragments of human complement receptor 2/CD21, Mol. Immunol. 46 (2009) 2630–2639.
[55] F. Santilli, N. Vazzana, L.G. Bucciarelli, G. Davi, Soluble forms of RAGE in human diseases: clinical and therapeutical implications, Curr. Med. Chem. 16 (2009) 940–952.